DYNAMIC PERFORMANCE OF A RADIAL WEAK POWER SYSTEM WITH MULTIPLE STATIC VAR COMPENSATORS

A. J. P. Ramos
Dept. de Movimento de Energia
CHESF, Recife, Brazil

H. Tyll
SIEMENS AG
Erlangen, Federal
Republic of Germany

ABSTRACT

This paper deals with the dynamic performance of a radial weak, heavily shunt compensated power system, with three Static Var Compensators (SVCs) of relatively large rating, installed at short distances from each other. Dynamic interactions between the SVCs control systems and between them and the network are analysed by using eigenvalues and frequency response techniques.

Some noteworthy effects concerning the SVCs' regulators' stability, that may arise in such systems, are here described. These effects, revealed in the eigenvalue analysis, were confirmed in TNA simulations. A brief description of the mathematical formulation and the complete system data are also included.

KEYWORDS: Thyristor Controlled Reactor (TCR), Eigenvalues, Frequency Response.

1. INTRODUCTION

Voltage control is certainly one of the most important problems in operating radial long transmission line systems. While steady-state voltage control or voltage regulation can be easily achieved with the conventional control devices such as switchable capacitors and reactors, transient voltage control requires faster and more effective means of control. In fact, severe overvoltages that may arise from rejection of concentrated load blocks, especially in radial weak power systems with large shunt capacitive compensation, must be rapidly controlled. This reduces stresses on system equipments and thus avoid risk of insulation breakdown.

To provide reactive power support and simultaneously an appropriate means of transient voltage control, three Static Var Compensators are being installed in a regional subsystem that is part of the interconnected Northern-Northeastern power system of Brazil. The first SVC is already in operation in the Fortaleza substation. The other two are being commissioned within the next eighteen months. A noteworthy feature of this system is the relatively large rating of the SVCs; 14%, 25% and 60% of the short-circuit power levels of the respective buses to which they are connected. Futhermore the electrical distances between the SVCs (Fig. 1) also contribute to provide this system with special dynamic characteristcs, where SVC regulator stability problem is of major concern. Some of the questions related to SVC regulator stability have been analysed by Larsen and Chow [1], using example systems. This interesting analysis focused on the problem essentially from the point of view of network resonances.

The purpose of this work is to provide insights into the dynamic interaction between the SVCs' control systems and between them and the network. Some cause-effect relations are studied and requirements for system component modelling are established. The limitations of the approach employed in the present paper are also commented on, and some further investigations in this direction are suggested.

89 WM 183-5 PWRS A paper recommended and approved by the IEEE Power System Engineering Committee of the IEEE Power Engineering Society for presentation at the IEEE/PES 1989 Winter Meeting, New York, New York, January 29 - February 3, 1989. Manuscript submitted January 29, 1988; made available for printing November 17, 1988.

2. BASIC CHARACTERISTICS OF THE SYSTEM UNDER STUDY

The present electric system, known as the Northern Subsystem, comprises three 230 kV transmission lines along 700 km from Paulo Afonso (bus B5 in Fig. 1) to the Fortaleza substation (bus B2 in Fig. 1). In this typical radial system, bus B5, which corresponds to the Paulo Afonso generating center, can be considered an infinite bus.

The three SVCs shown in Fig. 1 are composed of two sections, each one with one fixed capacitor and one TCR, both connected to 26kV buses (Fig. 3b). They can be operated with the two sections together in twelve-pulse operation mode, or with only one section, in six-pulse operation mode. The largest SVC, installed in Fortaleza, has been dimensioned so that it can draw from -140 Mvar (inductive) to +200 Mvar (capacitive) for any value of the HV busbar voltage (230 kV) within the voltage range ± 5% when operating with two sections, or from -70 Mvar to +100 Mvar when operating with only one section. The other two SVCs have equal ratings, from -70 Mvar to +100 Mvar with two sections, or from -35 Mvar to +50 Mvar with one section. They are being installed in the Milagres (bus B4) and Banabuiu (bus B3) substation.

In normal configuration, the system short-circuit power levels are aproximately equal to 570 MVA (B2), 680 MVA (B3) and 1200 MVA (B4). Therefore, the ratios between the short-circuit powers (Scc) and the SVC Control Range, known as the Effective Short Circuit Ratio (ESCR) [1] are equal to 1.67, 4.0 and 7.14 for the Fortaleza, Banabuiu and Milagres SVCs, henceforth referred to as SVCB2, SVCB3, and SVCB4, respectively. The ESCR plays an important role in the dynamic performance of the SVCs' control system stability and

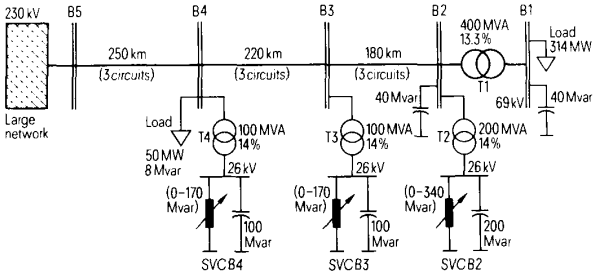

Fig. 1. Simplified one-line diagram of the Northern subsystem.

their interaction with the transmission system, as will be shown later.

3. EIGENVALUES AND FREQUENCY RESPONSE EVALUATION

3.1 General Comments

The construction of the system state matrix, the so-called A matrix, presents the major difficulty in state formulation, especially when generality, computational efficiency and arbitrary model flexibility are desired. Our present formulation was carried out in a way similar to that presented by Gross [4], so that the influence of each system component can be easily evaluated simply by manipulating the matrix A.

Among the different flexibilities provided by the developed program, two specific alternatives merit special attention: Instantaneous Mode (IM) formulation and Phasor Mode (PM) formulation. In IM formulation, the network dynamics is considered and the network differential equations are written in terms of Park Transformation based on lumped RLC circuits. The PM approach doesn't take the network dynamics into account, and makes use of the conventional complex algebraic load flow equations. This formulation is suitable for evaluating system dynamics when low frequency phenomena such as electromechanical oscillations are being analysed. These are cases in which the so-called stability programs apply.

3.2 Phasor Mode Formulation

System buses to which no loads or only impedance type loads are connected are eliminated by the usual kron method [10]. Buses to which dynamic elements, i.e., synchronous and induction machines, SVCs or non-linear loads are connected, are retained. For the reduced network, we can write [8]:

$$\Delta \mathbf{I}_{D,Q} = \mathbf{Y}_E \cdot \Delta \mathbf{V}_{D,Q} \qquad (1)$$

which is the nodal admittance equation expressed in the network frame of reference.

The set of first order and linear differential equations which correspond to synchronous and induction machines, to SVCs or dynamic loads [3] can be arranged so that, in compact form, we obtain

$$\mathbf{F} \cdot \dot{\Delta \mathbf{X}} = \mathbf{G} \cdot \Delta \mathbf{X} + \mathbf{H} \cdot \Delta \mathbf{I}_{D,Q} + \mathbf{P} \cdot \Delta \mathbf{U} \qquad (2)$$

where $\Delta \mathbf{X}$ is the state variable vector, $\Delta \mathbf{I}_{D,Q}$ is the injected current vector, $\Delta \mathbf{U}$ is the control variable vector, and **F**, **G**, **H** and **P** are matrices composed by the coefficients of the differential equations. For each retained bus we obtain a relationship between $\Delta \mathbf{I}_{D,Q}$ and $\Delta \mathbf{V}_{D,Q}$. For example, for synchronous machines, these relationships are the algebraic equations that result from stator differential equations when it is assumed that the flux derivatives are equal to zero. This equation set can be organised so that, in matrix form, it is written:

$$\Delta \mathbf{V}_{D,Q} = \mathbf{R} \cdot \Delta \mathbf{X} + \mathbf{S} \cdot \Delta \mathbf{I}_{D,Q} \qquad (3)$$

where **R** and **S** are coefficient matrices.

Eliminating $\Delta \mathbf{I}_{D,Q}$ and $\Delta \mathbf{V}_{D,Q}$ in (1), (2) and (3) yields the state space equation

$$\dot{\Delta \mathbf{X}} = \mathbf{A} \cdot \Delta \mathbf{X} + \mathbf{B} \cdot \Delta \mathbf{U} \qquad (4)$$

where

$$\mathbf{A} = \mathbf{F}^{-1} (\mathbf{G} + \mathbf{H} (\mathbf{I} - \mathbf{Y}_E \cdot \mathbf{S})^{-1} \cdot \mathbf{Y}_E \cdot \mathbf{R}) \qquad (5)$$

$$\mathbf{B} = \mathbf{F}^{-1} \qquad (6)$$

and **A** is the system state matrix, and **B** is the system control matrix.

3.3 Instantaneous Mode Formulation (IM)

In IM the network dynamics is considered. Elimination of the network voltages and node injected currents are not accomplished, since these variables are now state variable. Although conceptually simple, the IM is somewhat complex for arbitrary and general configurations. A detailed description of IM is presented in [3], in particular, with respect to the composition of the differential equations related to system components, and aimed at obtaining the state space equation form. The construction of the state matrix associated with the network makes use of the approach proposed in [6].

3.4 Frequency Response Evaluation

Once the control and system state matrices have been set up, the system frequency response relating output variables (vector **Y**), with control variables (vector **U**) can be easily evaluated from equation (4). It is derived in [3] and [7] and has the form

$$\Delta \mathbf{Y}(jw) = \mathbf{C} \cdot \mathbf{M} (jw\mathbf{I} - \Lambda)^{-1} \cdot \mathbf{M}^{-1} \cdot \mathbf{B} \cdot \Delta \mathbf{U} (jw) \qquad (8)$$

where **C** is the system output matrix, **M** is the eigenvector matrix, Λ is the diagonal eigenvalues matrix, **I** is the identity matrix, and w the angular frequency.

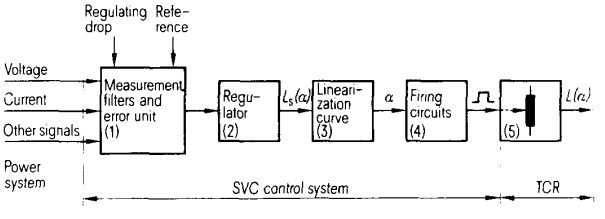

Fig. 2. Basic Structure of a SVC

3.5 Modelling the SVCs

Basic structure of the SVCB2, SVCB3 and SVCB4, comprising measurement, filters, error

units, regulators, linearization curve and firing circuit blocks, is shown in Fig. 2, where α is the thyristor firing angle and $L(\alpha)$ the resulting inductance effect.

Time simulation of electromagnetic transients requires extremely detailed modelling of the SVC, where each of above-mentioned are faithfully represented, so that the SVCs responses are appropriately reproduced. Models of the SVCB2, SVCB3 and SVCB4 for electromagnetic transient simulations implemented in the EMTP [9] are described in [5].

For balanced dynamic transient phenomena, only the effect of the thyristor switching process, in terms of fundamental frequency voltages and currents, is considered. Owing to this assumption, existing harmonic currents and voltages are not taken into account, and TCRs are represented as continuously variable admittances or as equivalent approaches, as that used by Hammad [2].

Judicious analysis of the complete control system circuits leads to the model

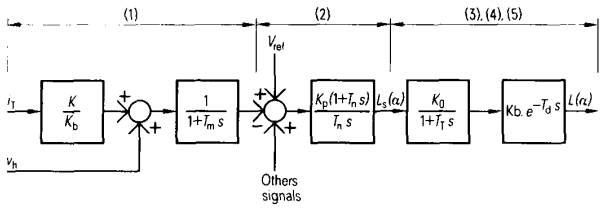

Fig. 3a. SVC Control System Model.

shown in the block diagram of Fig. 3a, where only the essential and functional elements associated with the dynamic phenomena to be studied are considered. The parameters of the SVCs control systems are presented in Appendix.

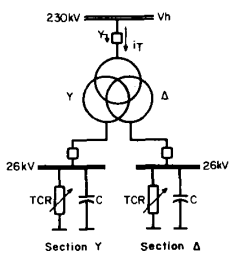

Fig. 3b. SVC Power Circuit.

4. SYSTEM DYNAMIC PERFORMANCE ANALYSIS

4.1 Network-SVC Interaction. Modelling Requirements.

Network reaction caused by an admittance change resulting from SVC regulator action is heavily dependent on several system parameters. In many cases, this cause-effect relationship can be quantified simply by the short-circuit power level or, more precisely, by the sensitivity coefficients relating voltage magnitude and admittance variations. These are cases of strong power systems for which oscillation frequencies associated with the network eigenvalues are significantly high, so that little or practically no dynamic interactions exist between the SVC control system and the network. The network here behaves as a "stiff" system.

On the other hand, a weak heavily shunt compensated power system, as is under consideration here, has low frequency oscillation modes that may interact with the SVCs' control systems to produce, under specific conditions, significant effects that are described below.

Analysis using the IM shows four eigenvalues associated with the SVC control system; two real, and one pair of complex eigenvalues that also become real when regulator gain is very low. The two real eigenvalues, one of which is due to the thyristor time delay Td, represent very fast-decaying non-oscillatory modes. They are practically insensitive to gain variations. The complex eigenvalues are strongly affected by regulator gain and hence determine system stability limits. Such eigenvalues, usually referred to as "dominant", are the primary focus of our analysis.

Figures 4a, 4b and 4c show how the dominant eigenvalues of the system are affected by SVC regulator gains. Examination of these Figures yields the verifications:

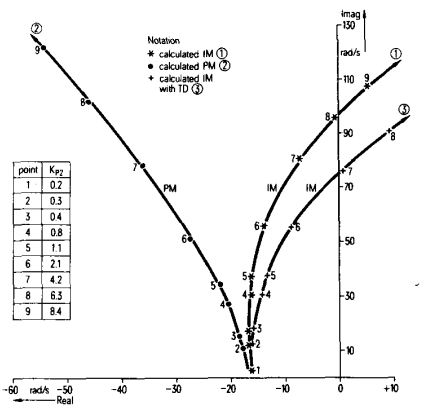

Fig. 4a. Loci of the dominant eigenvalues for different SVCB2 regulator gains. SVCB3 and SVCB4 in manual.

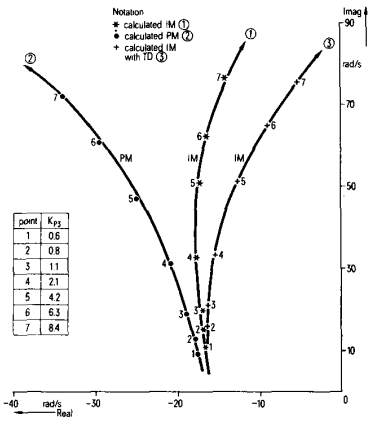

Fig. 4b. Loci of the dominant eigenvalues for different SVCB3 regulator gains. SVCB4 and SVCB2 in manual.

a - The oscillation frequency associated with the dominant eigenvalues increases with the regulator gain faster for the SVC with lower ESCR.

b - For a given regulator gain, the stability margin is lower for the SVC with lower value of ESCR. For instance, the stability limit is reached with Kp2 = 4.2 pu/pu for SVCB2. For SVCB4 this limit is reached for a gain greater than 21.0 pu/pu.

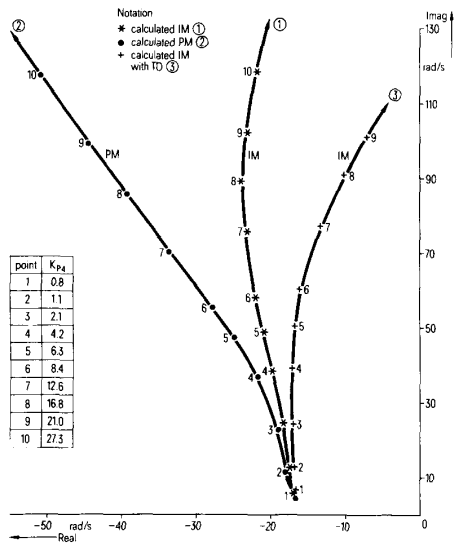

Fig. 4c. Loci of the dominant eigenvalues for different SVCB4 regulator gains. SVCB2 and SVCB3 in manual.

c - Up to approximately 5 Hz, the effect of the network dynamics on system stability is not yet significant.

d - For high oscillation frequencies, the tendency of the dominant eigenvalues depends on whether we take into account the network dynamics or not. This is why the use of conventional stability programs, where the network dynamics is not considered, can lead to false and dangerous results. This fact is especially important for systems with SVCs that have low ESCR and that make use of middle-to-high regulator gain.

e - The 5 Hz limit also seems adequate for indicating the maximum frequency for which the thyristor time delay Td may be disregarded.

For the system under study (Fig. 1), the lowest oscillation frequency associated with the network is about 100 Hz. In manual, admittances of the SVCs remain constant, equal to the initial values defined in the load flow and regulator actions are, obviously, not to be considered. It should be noted that operation of SVCB2 in automatic with a gain equal to 6.3 pu/pu produces a resonance at 15.4 Hz (Fig. 5), reflecting interaction between the SVCB2 control system and the network. This corresponds to point 8 on Curve 1 in Fig. 4a.

4.2 Effect of the SVC Operating Point

Figures 6a, 6b and 6c show the effect of the initial SVC operating point on system stability. It can be seen that operation with two sections (Curve 1) is less damped than operation with one (Curve 3), even with the same per-unit control loop gain, and with the same total reactive power injected into the HV busbar i.e., the SVC dispatch. This difference, which increases with regulator gain, is caused solely by the different initial operating point.

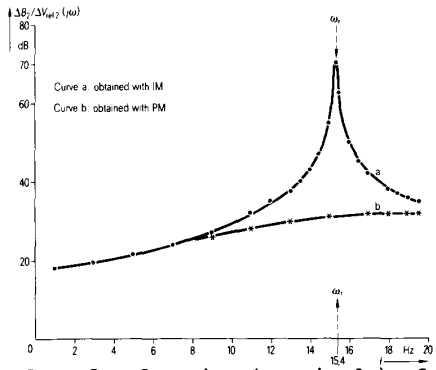

Fig. 5. Transfer function (magnitude) of SVCB2 with Kp2=6.3 pu/pu. SVCB3 and SVCB4 in manual.

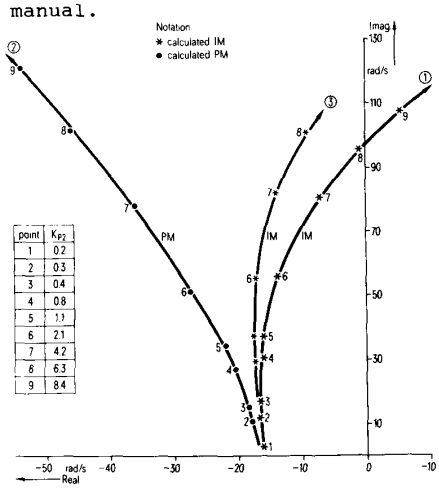

Fig. 6a. Loci of dominant eigenvalues for different values of Kp2. SVCB2 dispatch is equal to 60 Mvar capacitive. SVCB3 and SVCB4 in manual.

Curves 1, 2- Operation with two sections, fixed capacitors: 2x100 Mvar; TCRs 2x70 Mvar.

3- Operation with one section, fixed capacitor: 1x100 Mvar; TCR 1x40 Mvar.

In SVCs in the Northern subsystem, changing from one section to two section operation means duplicating the per-unit control loop gain, since regulator volt/volt gain remains unchanged. Consequently, there are two unfavourable effects that reduce the stability margin when the SVC mode is switched from six-pulse to twelve-pulse. For instance, operating at Kp2 = 2.1 pu/pu in six-pulse mode (Point 6 on Curve 3 in Fig. 6a), the switch to twelve-pulse operation means Kp2 = 4.2 pu/pu, which corresponds to point 7 on Curve 1 in Fig. 6a.

Comparison of the Fig. 6a, 6b and 6c shows that the above-mentioned dependence on the initial operating point is most significant for SVCB2, which has the lowest ESCR.

Analyses of several cases, with the system of Fig. 1, show that SVC operation in the inductive range is more damped than it is in the capacitive range. For SVCB2, this difference is more marked. These analyses were, clearly, IM analyses.

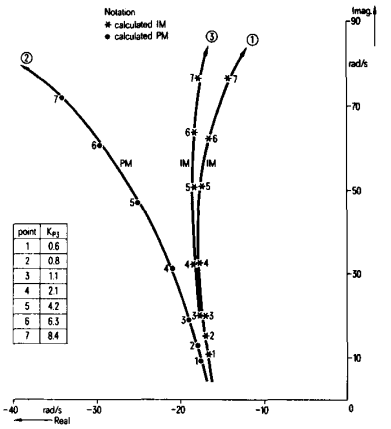

point	K_{p3}
1	0.6
2	0.8
3	1.1
4	2.1
5	4.2
6	6.3
7	8.4

Fig. 6b. Loci of dominant eigenvalues for different values of Kp3. SVCB3 dispatch equal to 30 Mvar capacitive; SVCB2 and SVCB4 in manual.

Curves 1, 2- Operation with two sections, fixed capacitors: 2x50 Mvar; TCRs: 2x35 Mvar.

3- Operation with one section, fixed capacitor: 1x50 Mvar; TCR: 1x20 Mvar.

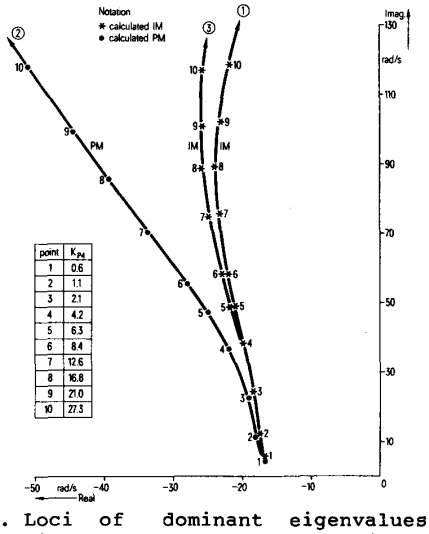

point	K_{p4}
1	0.6
2	1.1
3	2.1
4	4.2
5	6.3
6	8.4
7	12.6
8	16.8
9	21.0
10	27.3

Fig. 6c. Loci of dominant eigenvalues for different values of Kp4. SVCB4 dispatch equal to 30 Mvar capacitive; SVCB2 and SVCB3 in manual.

Curves 1, 2- Operation with two sections, fixed capacitors: 2x50 Mvar; TCRs 2x35 Mvar.

3- Operation with one section, fixed capacitor 1x50 Mvar; TCR 1x20 Mvar.

The aforementioned effects, detected with eigenvalues and frequency response analysis, were confirmed by TNA simulations. Figs. 7a and 7b show step response of SVCB2 operating in inductive and capacitive ranges, obtained in TNA simulations.

4.3 Operation With Two and Three SVCs

When two SVCs are in operation, three groups of eigenvalues associated with the SVC control systems are observed: a - four real eigenvalues, fast-decaying modes, insensitive to regulator gain variation; b - two eigenvalues that are complex for middle-to-high regulator gain, and whose oscillation frequency varies only slightly with regulator gain, and whose real part remains

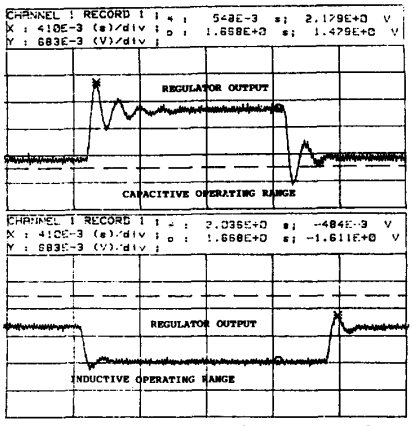

Fig. 7a. Step response of the SVCB2 operating in inductive and capacitive range.

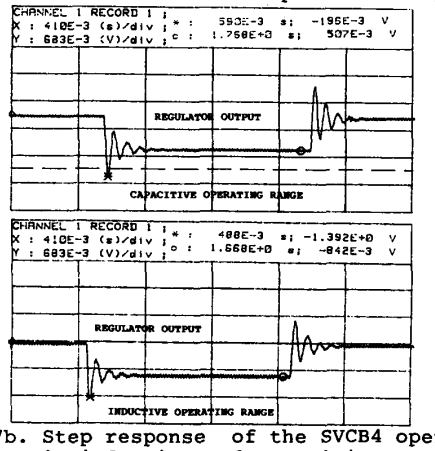

Fig. 7b. Step response of the SVCB4 operating in inductive and capacitive range.

almost constant; c - one pair of complex eigenvalues, strongly influenced by regulator gain. These are the dominant eigenvalues.

Loci of b and c eigenvalues for different values of Kp2 and Kp3, for SVCB2 and SVCB3 in automatic and SVCB4 in manual, are shown in Fig. 8. Similar features are observed when SVCB2 and SVCB4 (Fig. 9) and when SVCB3 and SVCB4 are in automatic mode.

The dominant pair of complex eigenvalues (group c) reflects interaction between the two operating SVCs. Each SVC influences this oscillation mode to an extent closely related to its corresponding regulator gain. The loci of the dominant modes of SVCB2 and SVCB3 when operating individually (Figs. 4a and 4b) are qualitatively similar, so that when operating simultaneously their individual characteristics appear to be added up, as shown in Fig. 8.

In case of automatic operation of SVCB2 and SVCB4, whose individual loci are somewhat different , the resultant dominant mode expresses the combination of two effects that, within a certain gain range, are opposite as Fig. 9 shows.

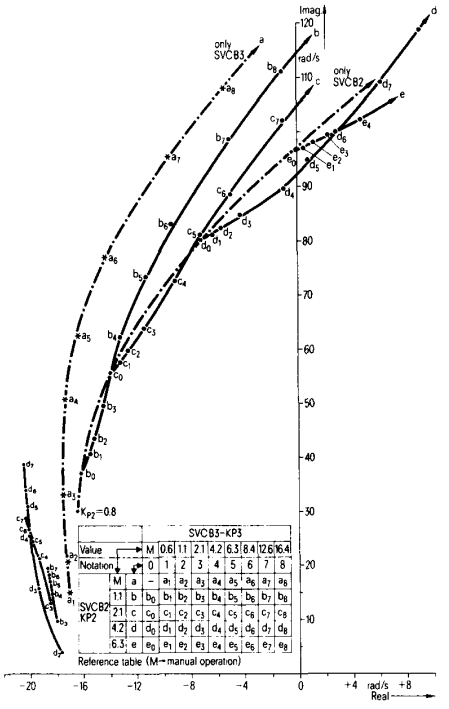

Fig. 8. Loci of dominant and group b eigenvalues for different values of Kp2 and Kp3. SVCB4 in manual.

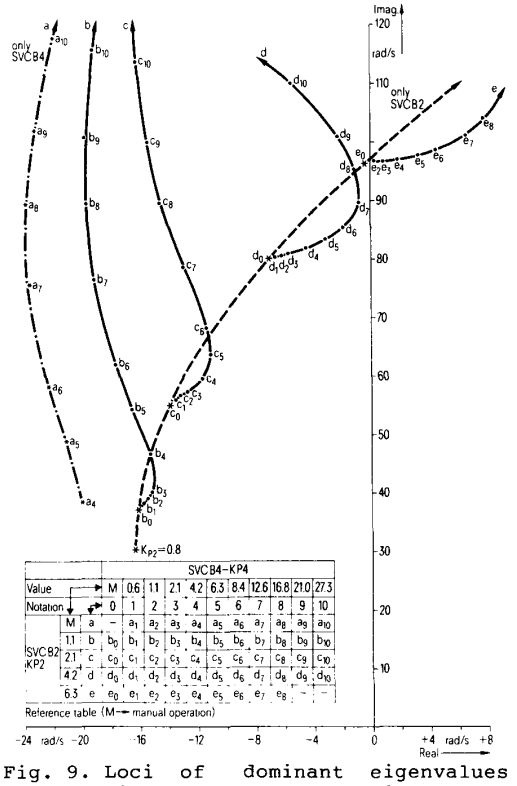

Fig. 9. Loci of dominant eigenvalues for different values of Kp2 and Kp4. SVCB3 in manual.

With Kp2 = 4.2 pu/pu, an increase in Kp4 at first contributes to instability. As Kp4 becomes greater than 12.6 pu/pu however, this tendency is reversed. This effect is also shown up in the frequency response analysis. Fig. 10 shows the Nyquist plot of SVCB2 in three conditions relating to points d0, d7 and d10 of Fig. 9, which correspond to curves a, b and c of Fig. 10.

System oscillation modes associated with three-SVC operation are very similar to those of two-SVC operation.

There is a group of six real eigenvalues that are very fast decaying modes; a group of two pairs of complex eigenvalues whose real

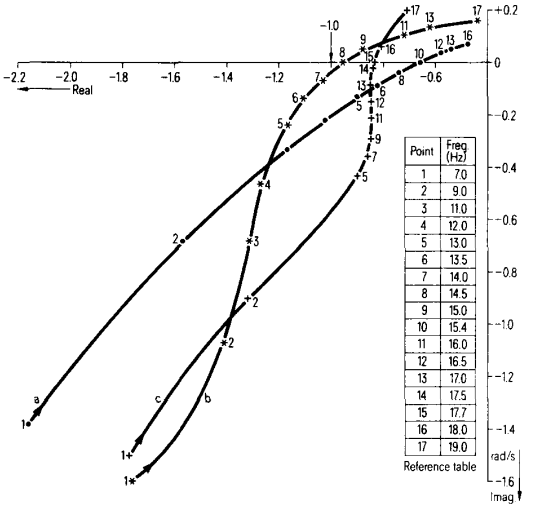

Fig. 10. SVCB2 open loop transfer function (Nyquist).
Curve a: Kp2 = 4.2 pu/pu, SVCB3 and SVCB4 in manual
Curve b: Kp2 = 4.2 pu/pu, Kp4 = 12.6 pu/pu, SVCB3 in manual
Curve c: Kp2 = 4.2 pu/pu, Kp4 = 27.3 pu/pu, SVCB3 in manual

parts are only slightly sensitive to regulator gain variations, and a pair of complex eigenvalues (dominants) that practically define system stability. The dominant oscillation modes are most sensitive to variations in Kp2, since SVCB2 has the lowest ESCR.

5. CONCLUSIONS

5.1 Operation of SVCs with low values of ESCR may exhibit oscillation mode frequencies above 5 Hz, depending substantially on SVC regulator gain. In such cases, both representation of network dynamics and thyristor time delay are crucial in the analysis of the SVC regulator stability limits.

5.2 Operation with two sections or with one section may present different dynamic performance, even when the same per-unit control loop gain is being used. This difference is more evident where ESCR is low, and increases with regulator gain. It has also been verified for the studied system that, for a given regulator gain, operation in the inductive range is more damped than operation in the capacitive range. Similarly, this effect is more

meaningful for cases of low ESCR and high regulator gain.

5.3 No sign of oscillations between SVCs have been noticed in multiple SVC operation. In all cases, a pair of complex oscillation modes determines system stability. These dominant eigenvalues are affected most by the SVC that has the lowest ESCR.

5.4 The present analysis is based on representing the TCR as a variable admittance. The highest frequency limit for which this assumption remains valid must be taken into consideration when detailed studies are being undertaken. Laboratory experiments with realistic SVC electronic models are currently under way. Preliminary results suggest 25 Hz as a reasonable limit.

6. ACKNOWLEDGEMENTS

The authors would like to thank Prof. G. Hosemann of Erlangen University and Dr. Dusan Povh of Siemens AG for their valuable suggestions and discussions. They would also like to acknowledge the financial support provided throught 1986 by the Alexander von Humboldt Foundation and the Krupp Foundation.

7. REFERENCES

1 - E. V. Larsen, J. H. Chow, "Application of Static Var Systems for System Dynamic Performance". IEEE Special Publication 87THO187-5-PWR.

2 - A.E. Hammad, M. El-Sadek, "Application of a Thyristor Controlled Var Compensator for Damping Subsynchronous Oscillations in Power Systems". IEEE, Trans vol. PAS-1Ø3/1, pp. 198-212, January 1984.

3 - A.J.P. Ramos, "Dynamic Performance of a Radial Long Transmission System with Multiple Static Var Compensators". University Erlangen, Report Ev-Bericht F227, March 1987.

4 - G.Gross, C.F. Imparato, P.M. Look, "A Tool for the Comprehensive Analysis of Power System Dynamic Stability". IEEE, Trans vol. PAS-1Ø1/1, pp. 226-234, January 1982.

5 - A.J.P. Ramos, J.S. Monteiro, H.D. Silva, "Detailed Modelling of Static Var Compensators for Electromagnetic Transient Simulations" (in portuguese). Presented at VIII SNPTEE, Group IV, São Paulo, Brazil, September 1986.

6 - E.S. Kuh, R.A. Rohrer, "The State-Variable Approach to Network Analysis". Proceedings of the IEEE, vol. 53, pp. 672-682, July 1965.

7 - E.V. Larsen, W.W. Price, "MANSTAB/POSSIM Power System Dynamic Analysis Program - A New Approach Combining Non-linear Simulation and Linearized State-Space/ Frequency Domain Capabilities". PICA, pp. 35Ø-358, 1977.

8 - J.M. Undrill, "Dynamic Stability Calculation for an Arbitrary Number of Interconnected Synchronous Machines". IEEE, Trans vol. PAS-87, pp. 835-844, March 1968.

9 - Rule Book, "Electromagnetic Transient Program (EMTP)". Bonneville Power Administration, Portland, 1984.

1Ø- H.E. Brown, "Solution of Large Networks by Matrix Methods". Book, John Wiley & Sons, Inc.

8. APPENDIX - System Data

. Transmission Lines - per circuit, 23Ø kV

r = Ø.Ø9 ohm/km, x = Ø.5Ø ohm/km,
y = 3.28E-6 S/km, 23Ø kV.

. Transformers (taps = 1.Ø) and loads (constant impedance type): indicated in the Fig. 1.

. SVC data

SVC	Kb	Kp(pu/pu)	Tn(s)	SR(MVA)
SVCB2	3.4	2.1	Ø.Ø1	34Ø.
SVCB3	1.7	2.1	Ø.Ø1	17Ø.
SVCB4	1.7	2.1	Ø.Ø1	17Ø.

Kb = SR/Sb
SR - TCR rating (MVA); Sb - System base (MVA). Here, Sb = 1ØØ MVA. Ko = 1.Ø, T_T = Ø.ØØ46s, K = Ø.Ø1pu,(referred to SR) Tm = Ø.Ø3s, for the SVCB2, SVCB3 and SVCB4.

. Initial operating point (base case):

BUS	VT(pu)	Ang(degree)	Cap/Ind(+/-)
B5	1.Ø2	Ø.Ø	Ø.
B1	1.Ø2	-5Ø.Ø	Ø.
B2	1.Ø15	-44.Ø	Ø.
SVCB2	1.Ø25	-44.Ø	1Ø.5
B3	1.Ø18	-33.1	Ø.
SVCB3	Ø.997	-33.1	-14.9
B4	1.Ø1Ø	-19.1	Ø.
SVCB4	Ø.989	-19.1	-14.7

ÁLVARO JOSÉ PESSOA RAMOS was born in Recife, Brazil, in 1951. He received the B.S degree in Electrical Engineering from the Federal University of Pernambuco, Brazil in 1973, and the M.Sc from the Federal Engineering School of Itajubá, Brazil in 1975. From March/1986 to March/1987 he was at the University Erlangen Federal Republic of Germany and at the High Voltage Transmission Engineering Department of Siemens AG for a research program. In 1974 he joined CHESF, Recife, Brazil, where he is engaged on system stability and system dynamic problems. He is member of the IEEE.

HEINZ TYLL was born in Hof, Bavaria, Federal Republic of Germany on May 15, 1947. In 1968 he was graduated in Electrical Engineering from the Coburg Polytechnikum. In 1974 he received the diploma degree from the Technical University of West-Berlin. After starting work with Siemens AG, he subsequently joined their High Voltage Transmission Engineering Departament, where he has been employed since 1975. He is responsible for SVC design and Transmission System Analysis.

Discussion

E. M. de Oliveira (Centro de Pesquisas de Energia Elétrica, CEPEL, Rio de Janeiro, Brazil): The paper presents very relevant aspects related to the dynamic characteristics on the voltage control process by SVC's applied to weak transmission systems. It's shown that the instability of the dominant oscillatory mode is possible and verified in computational simulations only when transmission system positive sequence is properly represented. Inclusion of Ldi/dt and (1/C) idt types of voltage components on the expression relating network dq voltages and currents is, therefore, necessary, taking into account the relatively high values possible to be assumed by the frequency of the referred dominant oscillatory mode when compared to the frequencies associated with the electromechanical instability phenomeon (in range of 0.2 to 3.0 hz). In case of weak systems, detailed network modelling is also imperative, such that to avoid high unaccuracy in the evaluation of dominant mode characteristics. This mode is responsible by possible instability on the voltage control dynamic process due to SVC'S.

The authors emphasize the need of SVC'S control system detailed representation, especially when utilizing high regulator gain Kp. It's also shown that increase in this gain is restricted by the instability of the dominant mode. Figure 9 is particularly interesting since it shows the excursion of this mode (considering control operations of SVCB2 and SVCB4 on automatic mode) as a function of increase on gains K_{p2} and K_{p4}. Feasible increases on K_p are naturally smaller for the lower effective short circuit ratio SVC.

I would appreciate if the authors, based on others simulations not referred in the paper, make comments with respect to the effect of different system reactive requirement distribution between the SVCS. Only one base operating condition is mentioned in the paper. Perhaps an appropriate reactive power distribution between the SVCS allows a further increase on gain K_{p2} without instability of the dominant mode.

Comments on the effect of different load representation in the receiving system (bus B1) and about how time delay $e^{-\tau d \cdot S}$ was represented in the space state linearized treatment for eigenvalue calculations are also appreciated.

Finally I would like to commend the authors of this very informative paper.

Manuscript received February 22, 1989.

A. E. Hammad (ABB Power Systems, Baden, Switzerland): The authors are to be commended for a very interesting paper that deals with important and timely topics in the field of SVC applications.

1. In my opinion the paper has correctly answered the question of interaction between SVC's in multiple SVC system operation. Have the authors done any field measurements (or TNA simulations) that confirms their results?
2. The observation about the validity of the results obtained using quasi steady state phases representation (PM) is very important. It emphasizes the point of the danger in misusing the conventional transient stability programs for modeling fast dynamics on account of components such as SVC or HVDC systems [A]. As the authors correctly point out, such discrepancies are more pronounced as the SCR is lower—which is the normal case where SVC or HVDC system applications are mostly desired. Have the authors made any time simulations to show such discrepancies?
3. In all studies involving SVC and HVDC applications where problems of high frequency (greater than 10% fo) are investigated (such as transient voltage instability and sub synchronous or low order harmonic resonances), we have used a systematic approach based on system data of conventional stability programs for arbitrary and general configurations but taking network dynamics into consideration [B]. We found that the conversion from PM to IM is relatively easy and efficient. The wide spectrum of eigenvalue and frequency domain analysis provided us with deep understanding and realistic solutions for such problems [C]. We are also planning to report on some of these results in the near future. In this regard, a comment from the authors regarding their current work on suitable TCR models for higher frequencies will be appreciated.

References

[A] J. Reeve, R. Adapa, "Evaluation of Developments in DC Models for ac/dc Transient Stability Programs", CIGRE Symposium: AC/DC Transmission Interactions and Comparisons. Boston, Sept. 1987, Paper 100-04

[B] A. Hammad, M. El-Sadek, "Prevention of Transient Voltage Instabilities due to Induction Motor Loads by Static Var Compensators", IEEE PES Winter Meeting 1989, Paper No. 89 WM 149-6 PWRS.

[C] A. Hammad, L. Pilotto, "Thyristor Phase Regulated Transformers, An Advanced Approach for Damping Torsional Interactions", IEE Int. Conference on AC & DC Power Transmission, London, Sept, 1985, IEE Pub. Nr. 255, pp. 69-74.

Manuscript received February 20, 1989.

Álvaro J. P. Ramos and **H. Tyll**: The authors would like to express their appreciation to the discussors for their valuable comments. Addressing first to the points raised by Dr. A. Hammad in the order in which they are presented:

1. Field measurements were not yet done because only the first SVC (SVCB2) is in operation. The second SVC (SVCB4) will be in operation until June/1989. Some field measurements are scheduled to be carried out immediately after the SVCB4 commissioning. We don't expect, however, that these field measurements will be able to provide sufficient information to confirm the results concerned with the SVC's interactions reported in the paper. Due to the use of relative small regulator gains, the SVC responses are highly damped, so that the verification of eventual oscillation between the SVCs are not possible. However, EMTP [9] time simulations, with a three-phase detailed SVC model, where firing and synchronizing circuits are appropriately represented, have been utilized to confirm the effects predicted by eigenvalue/ eigenvector analysis. The table below shows the complex eigenvalues associated with the SVC controllers, in relation to the operation of SVCB2, SVCB3 and SVCB4 in automatic mode. While the eigenvalue b is only slightly sensitive to regulator gain variations, eigenvalue a is the dominant, sensitive to regulator gain variation and thus determine, system stability. The table also presents the eigenvector components corresponding to SVC regulator output variables (UR2, UR3 and UR4) related to eigenvalues a and b.

EIGENVALUE	EIGENVECTOR ELEMENTS		
	UR2	UR3	UR4
a)- 6.0±j44.4	0.4/-36°	0.9/-34°	0.5/-36°
b)-18.2±j13.2	0.8/-20°	1.0/-17°	1.9/+159°

With respect to eigenvalue a, time responses (regulator ouputs) of SVCB2, SVCB3 and SVCB4 are practically in phase, i.e, there is no reactive power oscillation between the SVCs. It should be noted that eigenvalue a is the dominant and constitutes the oscillation mode that is more evident with time response analysis. On the other hand, regarding to eigenvalue b, the eigenvector analysis shows that SVCB2 and SVCB3 oscillate almost in phase but in counterphase with respect to SVCB4. This fact is not clearly noticeable with time simulation analysis due to the predominance of oscillation mode a. Fig. 1 presents the SVC's time responses for a three-phase short-circuit applied to bus B3 through a reactance with duration equal to 10ms. This time simulation

confirms the results obtained with eigenvalue/ eigenvector analysis.

2. Fig. 2 presents the SVCB2 step response for different values of Kp2, obtained with a stability program (PM formulation). It is also presented the same simulation (exactly same condition and parameters) carried out with the EMTP, where the thyristor switching process is represented in detail. The discrepancies, as predicted by eigenvalue analysis, become larger for high values of regulator gains.

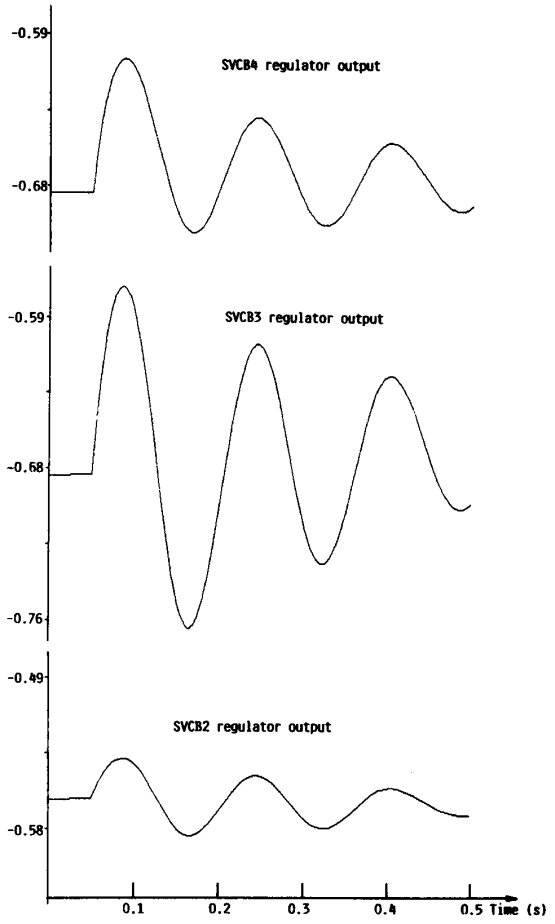

Fig. 1 - SVC's regulator time response for a three-phase short-circuit in "per-unit".

Time simulations obtained with a stability program and PM eigenvalue analysis have shown a good agreement for all studied conditions, and for all studied regulator gains. The comparison between EMTP time simulation and IM eigenvalue analysis however, demonstrates that significant high discrepancies occurs when large SVC regulator gain are used. These are conditions for which high frequency oscillation modes are present and TCR model is not reliable. It must be mentioned that, for all studied cases, EMTP time simulations yield less damped results and hence lower stability margins.

3. The TCR is the most difficult element to be represented in a linear analysis. The frequency limit to which a linear representation is still valid is not yet completely clear. It seems to us that the experience obtained with the comparison between linear analysis and time simulations with detailed TCR modeling, for a specific system, is very important. Frequency response tests, obtained in laboratory with an electronic model of SVC control circuits can also provide insights into this question.

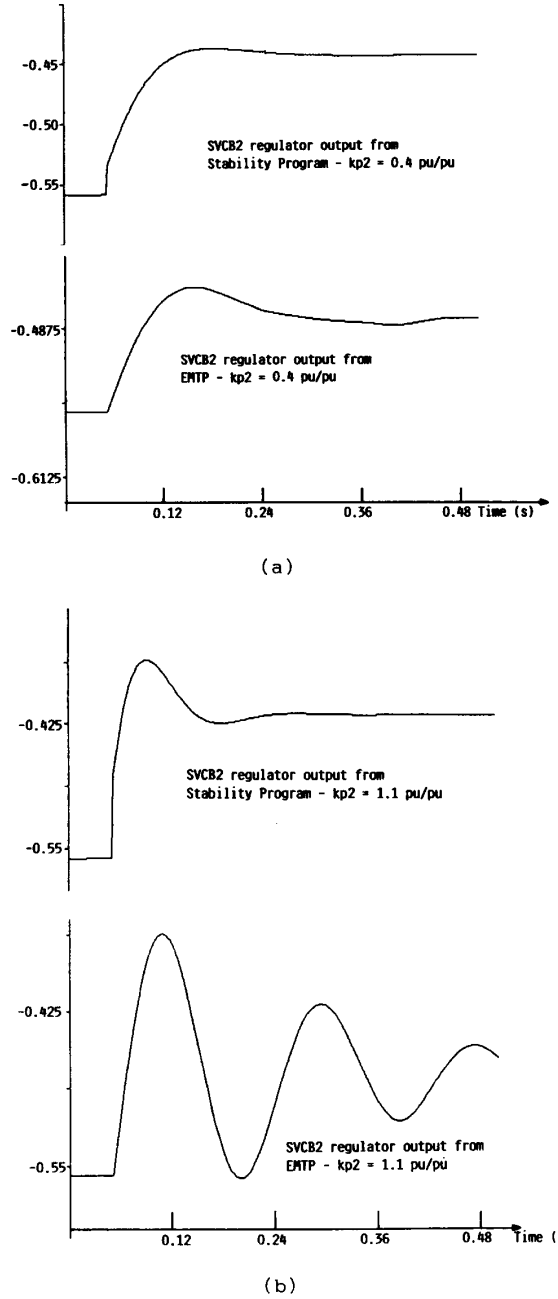

Fig. 2 - SBC2 step responses in "per-unit".

A frequency response experiment was carried out with a TCR electronic model connected to an ideal voltage source. The regulator output is disconnected and the linearization curve circuit is fed by a sinusoidal voltage signal which has a known combination of 5 hz and 15 hz. The thyristor current and the input signal are shown in Fig. 3. A spectral analysis shows that the TCR gains (UO/UI), for 5 Hz and 15 Hz, remain unaffected if compared with the cases where 5 Hz and 15 Hz signals are applied

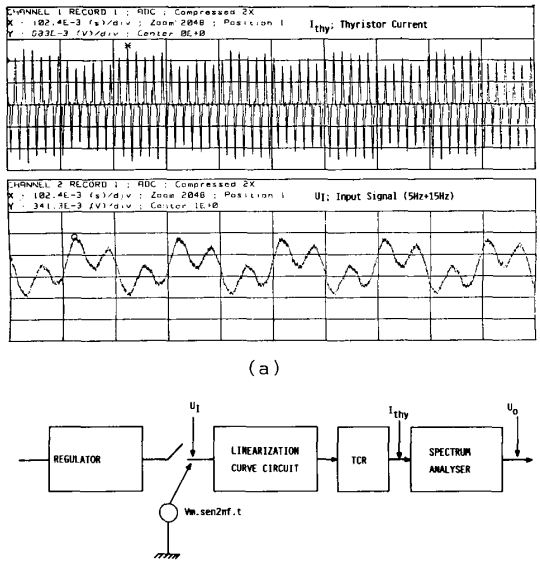

Fig. 3 - TCR frequency response experiment

separately. This is an indication that the superposition principle applies for this frequency range and the TCR linear model may be still acceptable.

Our comments on the points raised by Dr. Sebastião E. M. de Oliveira are as follows:

We didn't investigate the specific question of reactive power distribution between the SVCs. It seems to us that variation on reactive power distribution between SVCs may affect system dynamic performand as much as network oscillation modes are accordingly modified. As mentioned in the paper, for large Kp2, SVCB2 operation in the inductive range is more damped than the operation in the capacitive range. Also, for the same SVCB2 dispatch, different dynamic performances are observed for six pulse operation mode and twelve pulse operation mode. These are situations that demonstrate the effect of SVC operating point on system dynamic performance as a result of the corresponding change in network oscillation modes.

The nature of the load plays an important role on system dynamic performance especially when a significant dynamic characterist is of concern, as is the case of induction motor loads. The results reported in the paper, however, are obtained with impedance type load.

The representation of thyristor time delay made use of the approximation:

$$e^{-Td.s} = G(s) = \frac{1 - Ts}{1 + Ts}, \qquad \text{where } T = Td/2$$

G(s) has frequency independent gain, equal to unity, and a phase shift practically equal to that of the time delay function for frequencies up to 40 Hz, as shown in Fig. 4. For such a frequency limit, the TCR modeling is no longer valid, so that this approximation doesn't represent any additional limitation.

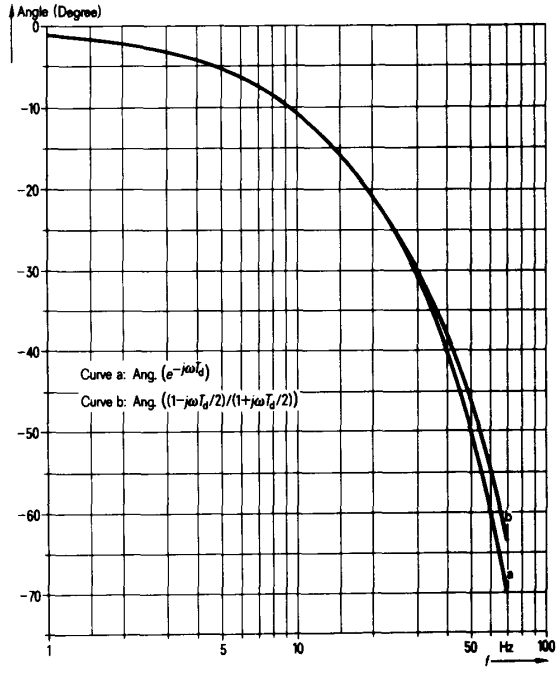

Fig. 4 - Time delay and G(s) phase variation with frequency.

Manuscript received April 24, 1989.